Inorganic Chemistry

Article

pubs.acs.org/IC

Thorium Fluorides ThF, ThF_2, ThF_3, ThF_4, $ThF_3(F_2)$, and ThF_5^- Characterized by Infrared Spectra in Solid Argon and Electronic Structure and Vibrational Frequency Calculations

Lester Andrews,*[,†] K. Sahan Thanthiriwatte,[‡] Xuefeng Wang,[†] and David A. Dixon*[,‡]

[†]Department of Chemistry, University of Virginia, Charlottesville, Virginia 22904-4319, United States

[‡]Department of Chemistry, The University of Alabama, Shelby Hall, Tuscaloosa, Alabama 35487-0336, United States

Supporting Information

ABSTRACT: Reactions of laser-ablated Th atoms with F_2 produce ThF_4 as the major product based on agreement with matrix spectra recorded of the vapor from the solid at 800−850 °C. Weaker higher-frequency bands at (567.2, 564.8), (575.9, 575.1), and (531.0, 528.4) cm^{-1} in argon are assigned to ThF, ThF_2 and ThF_3, $ThF_3(F_2)$ on the basis of their chemical behavior upon increasing reagent concentrations, annealing, and irradiation, the use of NF_3, OF_2, and HF as F-atom sources, and a comparison with frequencies calculated at the DFT/B3LYP and CCSD(T) levels with a large segmented + ECP basis set on Th and the aug-cc-pVTZ basis set on F. An additional broader band at 460 cm^{-1} is assigned to the ThF_5^- anion. The trigonal-bipyramidal ThF_5^- anion (calculated electron detachment energy of 7.17 eV) increases at the expense of $ThF_3(F_2)$ and F_3^- on full mercury arc irradiation. $[ThF_3^+][F_2^-]$ is shown by calculations to be an ionic complex with a side-bound F_2^- subunit. This paper reports the first evidence for novel pentacoordinated thorium species including the unique $[ThF_3^+][F_2^-]$ ionic radical-ion pair molecule and its electron-capture product, the very stable ThF_5^- anion.

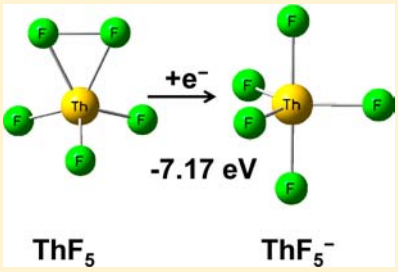

INTRODUCTION

Uranium hexafluoride is the basis for the important uranium isotope separation process by gaseous diffusion.[1] The UF_6 molecule is also interesting in its own right for vibrational spectroscopy (laser isotope separation)[2] and its large electron affinity with values of 4.9 ± 0.5,[3] >5.1,[4] and 5.3 eV.[5] However, the corresponding highest thorium fluoride, ThF_4, has received much less attention. The vapor in equilibrium with solid ThF_4 at 1200 °C exhibited an IR band at 520 cm^{-1}, which was assigned to the antisymmetric Th−F stretching mode.[6] Spectra of the vapor generated from the solid at 800−850 °C and trapped in argon and neon matrixes produced matrix site-split bands in the 520 cm^{-1} region.[7] Vapor-pressure data for thorium tetrahalides support the tetrahedral structure expected for the 4+ oxidation state of Th.[8] A high-resolution spectroscopic investigation of ThF and ThF^+ together with high-level electronic structure calculations has recently appeared.[9] The gaseous species ThF, ThF_2, ThF_3, and ThF_4 have been generated in a heated effusion beam source and observed as cations by mass spectrometry.[10]

The laser-ablation technique has been employed to generate both Th and U atoms for reactions with small molecules and to trap the novel intermediate reaction products in noble gas solids in this laboratory. Most recently, we have investigated the OUF_2 and $OThF_2$ molecules with polarized triple oxo bond character from reactions with OF_2.[11] Earlier work provided characterization of N−ThF_3, thorium oxides, the NThO molecule, and thorium hydrides.[12−15]

RESULTS AND DISCUSSION

IR spectra recorded from the reaction products of laser-ablated Th atoms codeposited with molecular fluorine (F_2) using established experimental methods[16−19] are illustrated in Figure 1 for 0.5% F_2 (scans a−d) and 1.0% F_2 (scans e−h). First, the strong absorptions at 521.0, 519.2, and 514.5 cm^{-1} in the region of the 520 cm^{-1} gas-phase absorption for ThF_4 are in agreement with argon matrix spectra of ThF_4 vapor from the solid at 800−850 °C.[6,7] New absorptions of interest here are the unresolved doublet at (575.9, 575.1) cm^{-1}, the resolved doublet at (567.2, 564.8) cm^{-1}, the 531.0 cm^{-1} band, and the 528.4 cm^{-1} band, which survives 20 K annealing, decreases upon >220 nm irradiation, and increases slightly upon final 30 K annealing. Meanwhile, absorption appears at 460 cm^{-1} upon deposition, decreases upon 20 K annealing, increases slightly and sharpens upon >220 nm irradiation, and decreases again upon final 30 K annealing. The F_3^- absorption at 510 cm^{-1} is destroyed by >220 nm irradiation.[19] Note the reversal of the 531.0 and 528.4 cm^{-1} band intensities with increasing F_2 concentration, where more F_2 favors the lower frequency band.

Additional laser-ablated thorium experiments were done in collaboration with the Riedel group at Freiburg using higher fluorine concentrations. Spectra for 2% F_2 in argon are illustrated in Figure SI-1 in the Supporting Information. Several points in comparison with the 1 and 2% F_2 experiments are noteworthy: (1) the same absorptions were observed within 0.1

Received: May 3, 2013
Published: June 27, 2013

   dx.doi.org/10.1021/ic401107w | Inorg. Chem. 2013, 52, 8228−8233

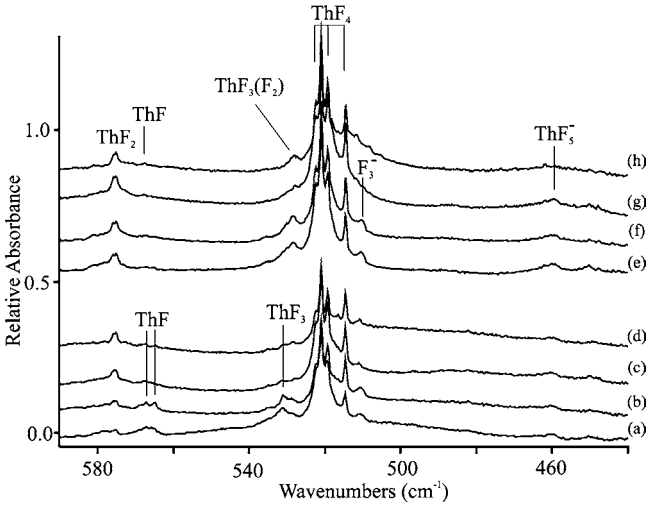

Figure 1. IR spectra of laser-ablated Th atom and F_2 molecule reaction products in solid argon: (a) Th + 0.5% F_2 deposition for 60 min; (b) after annealing to 20 K; (c) after $\lambda > 220$ nm irradiation; (d) after annealing to 20 K [spectra absorbance scale expanded two times]; (e) Th + 1% F_2 deposition for 60 min; (f) after annealing to 20 K; (g) after $\lambda > 220$ nm irradiation; (h) after annealing to 30 K.

cm^{-1}; (2) the 528.4 cm^{-1} band was slightly stronger than the 530.1 cm^{-1} band, photolysis destroyed them both, and annealing restored only the 528.4 cm^{-1} band; (3) the 460 cm^{-1} absorption was stronger, and it increased upon UV irradiation.

IR spectra using the NF_3 reagent instead of F_2 are shown in Figure 2 (scans a–e). As reported previously,[12] the major N–

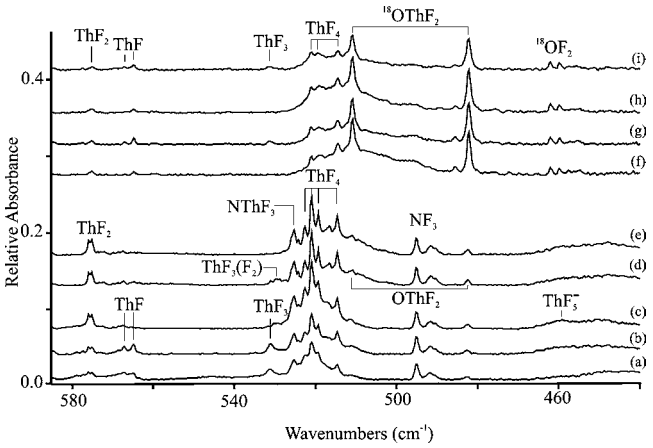

Figure 2. IR spectra of laser-ablated Th atom and NF_3 or OF_2 molecule reaction products in solid argon: (a) Th + 0.4% NF_3 deposition for 60 min; (b) after annealing to 20 K; (c) after $\lambda > 220$ nm irradiation; (d) after annealing to 30 K; (e) after $\lambda > 220$ nm irradiation. (f) Th + 1% $^{18}OF_2$ (91% enriched) deposition for 60 min; (g) after annealing to 20 K; (h) after $\lambda > 220$ nm irradiation; (i) after annealing to 30 K.

ThF_3 product can clearly be identified, and its strongest band, the antisymmetric ThF_3 stretching mode, appeared at 525.3 cm^{-1}. Here, we note first that exactly the same frequency, but weaker bands, was observed for ThF_4, and for the new products at (575.9, 575.1), at (567.2, 564.8), and at 531.0 cm^{-1}. Annealing to 20 K increased the latter three band groups slightly with the (567.2, 564.8) cm^{-1} peaks increasing more. Full mercury arc irradiation substantially decreased the (567.2, 564.8) cm^{-1} and 531.0 cm^{-1} peaks, doubled the intensity of the new (575.9, 575.1) cm^{-1} and ThF_4 bands, and enhanced a weak absorption at 460 cm^{-1}. Next annealing to 30 K slightly increased the 567.2 and 531.0 cm^{-1} peaks and a 528.4 cm^{-1} satellite feature and decreased the lower-frequency band, as observed with the F_2 reagent. A final >220 nm irradiation enhanced the broad 460 cm^{-1} absorption. The weak 511.1 and 482.3 cm^{-1} peaks are due to $OThF_2$ owing to the trace ThO impurity in the system.[11]

Matrix spectra from the reaction of Th with $^{18}OF_2$ are illustrated in Figure 2 (scans f–k), which includes regions not illustrated previously.[11] As reported, weaker bands were observed for ThF_4 and stronger new bands at 510.8 and 482.1 cm^{-1} for the major $^{18}OThF_2$ product.[11] Additional weak bands were observed at 575.2, 567.2, 564.8, 531.0, and 528.2 cm^{-1}. The (567.2, 564.8) cm^{-1} peaks and the major product bands increased upon annealing to 20 K, as before. Full arc photolysis increased the 575.2 cm^{-1} band and decreased the other weaker peaks. A final annealing to 30 K restored some of the 564.8 cm^{-1} band intensity. In this case, features in the 460 cm^{-1} region show small oxygen isotopic shifts and are due to the precursor and its aggregates.[11] It is significant that the 575.2, 567.2, 564.8, 531.0, and 528.2 cm^{-1} product bands did not shift in a similar experiment with Th and natural isotopic OF_2. Hence, their observation from Th reactions with F_2, NF_3, and OF_2 with no O-18 shift shows that these are due to molecular thorium fluoride species.

Additional chemical support can be derived from the fact that the same 576, 575, 567.2, 564.8, and 531.0 cm^{-1} absorption peaks were observed with the same annealing and photolysis behavior in analogous argon matrix experiments with Th and HF performed at Freiburg. Spectra from an HF experiment are shown in Figure SI-2 in the Supporting Information for comparison.

Evidence will be presented for the identification of thorium fluoride molecules in the order of increasing numbers of F atoms. The experimental assignments together with our computational results are given in Tables 1 and 2. First, the two sharp bands at 567.2 and 564.8 cm^{-1} and a weaker matrix site splitting at 569.2 cm^{-1} can be assigned to the ThF molecule. These bands are photosensitive, and they are restored upon annealing, more than any other new product bands in this system. Thus, a straightforward reaction must be available to form this product, and that reaction is the direct exothermic combination of atoms to form ThF, whose energy is given for reaction 1 in Table 3.[9,10] UV irradiation by the laser-ablation plume provides F atoms from precursor photodissociation. Second, these bands are observed with the F-atom precursors NF_3, OF_2, and HF with relative product band intensities even more prominent than those with F_2 itself. Third, an approximate gas-phase fundamental of 605 ± 15 cm^{-1} was deduced from electronic band spacings, which is in reasonable agreement with a multireference configuration interaction calculation (574 cm^{-1}).[9] Fourth, our calculations[20,21] at the spin-unrestricted density functional theory (DFT) level with the B3LYP exchange-correlation functional[22,23] and at the correlated molecular orbital theory coupled cluster CCSD(T)[24−27] level produce frequencies in this region appropriately slightly higher than the above argon matrix values and consistent with the experimental gas-phase result (Table 1). [R/UCCSD(T) has a restricted open-shell Hartree–Fock calculation for the starting wave function with the spin

dx.doi.org/10.1021/ic401107w | Inorg. Chem. 2013, 52, 8228−8233

Table 1. Calculated Thorium Fluoride Geometry Parameters, Frequencies (cm^{-1}), IR Intensities (km/mol), and Observed Argon Matrix Frequencies (cm^{-1})

parameter	CCSD(T)/aug-cc-pVTZ/ECP	B3LYP/aug-cc-pVTZ/ECP[a]	obsd[b]
	ThF($^2\Delta$)		
r(Th−F) (Å)	2.0319	2.037	
Th−F str	598.9[c]	587.2 (78)[a]	567.2, 564.8, (605 ± 15)[d]
	ThF_2(C_{2v} $^1A_1$)		
r(Th−F) (Å)	2.061	2.061	
∠(F−Th−F) (deg)	129.2	142.3	
F−Th−F bend (a_1)	67.1	106.1 (2)	
Th−F sym str (a_1)	585.4	581.8 (17)	
Th−F asym str (b_1)	573.4	577.2 (186)	575.1, 575.9
	ThF_3(D_{3h} $^2A_1$)		
r(Th−F) (Å)	2.103	2.105	
out-of-plane bend (a_2'')	28.5	65.6 (5)	
F−Th−F bend (e')	105.6	96.9 (20)	
Th−F asym str (e')	537.2	539.3 (394)	531.0
Th−F sym str (a_1')	570.8	571.9 (0)	
	ThF_4(T_d $^1A_1$)		
r(Th−F) (Å)	2.117	2.112	
F−Th−F asym bend (e)	112.0	101.7 (0)	
Th−F sym bend (t_2)	113.2	93.9 (90)	
Th−F asym str (t_2)	528.3	537.5 (627)	521.0, 519.2, 514.5
Th−F sym str (a_1)	563.3	588.6 (0)	

[a]IR intensity (km/mol) in parentheses. [b]Argon matrix frequencies. [c]$\omega_e x_e$ = 2.1 cm^{-1}. [d]Gas phase.[9]

constraint relaxed in the coupled cluster calculation where both use the aug-cc-pVTZ basis set on F[28] and the small-core relativistic effective core potential (ECP) from the Stuttgart group with a corresponding segmented basis set on Th.[29] We denote this basis set as aug-cc-pVTZ/ECP.] The CCSD(T) calculations correlated 12 electrons on Th and 7 electrons on F. Furthermore, the CCSD(T) harmonic value for the asymmetric Th−F stretch of ThF_4 is within 8 cm^{-1} of the experimental anharmonic matrix value (Table 1). The calculated bond dissociation energy for ThF requires a spin−orbit correction of 8.8 kcal/mol for the Th atom[30] and a correction of 0.38 for the F atom.[31] The site-split ThF_4 absorptions were 8 cm^{-1} higher in solid neon than argon,[7] so we expect a higher neon matrix value for ThF. From these observations, we predict a gas-phase fundamental in the 580−600 cm^{-1} range, which is in accordance with the calculations and the estimate from the band structure.[9]

The matrix site-split doublet at (575.9, 575.1) cm^{-1} observed in all experiments with F_2, NF_3, OF_2, and HF increased slightly in intensity upon 20 K annealing and increased substantially in intensity upon photolysis. This band is the most prominent product after ThF_4. Our CCSD(T)/aug-cc-pVTZ/ECP calculation predicts a C_{2v} $^1A_1$ state to be the ground state for ThF_2 and the strongest mode, the antisymmetric stretch, to be within

Table 2. Calculated ThF_4^-, $[ThF_3^+][F_2^-]$, and ThF_5^- Geometry Parameters, Frequencies (cm^{-1}), and IR Intensities (km/mol), and Observed Argon Matrix Frequencies (cm^{-1})

parameter	CCSD(T)/aug-cc-pVTZ/ECP	B3LYP/aug-cc-pVTZ/ECP[a]	obsd
	ThF_4^-(D_{4h} $^2A_{1g}$)		
r(Th−F) (Å)	2.180	2.179	
Th−F sym str (a_{1g})	511.1	504.0 (0)[a]	
Th−F asym str (e_u)	456.4	452.5 (503)	
Th−F asym, sym str (b_{1g})	428.3	418.4(0)	
	ThF_4^-(T_d $^2A_1$)		
r(Th−F) (Å)	2.149	2.161	
Th−F sym str (a)		511.7(0)	
Th−F asym str (t)		481.8 (268)	
	$[ThF_3^+][F_2^-]$(C_s $^2A''$)		
r(Th−F_{bonded}) (Å)	2.106	2.108	
r(Th−$F_{nonbonded}$) (Å)	2.356	2.363	
r($F_{nonbonded}$−$F_{nonbonded}$) (Å)	1.908	1.962	
∠F_{bonded}−Th−F_{bonded} (deg)	106.6/101.5	108.4/102.1	
∠$F_{bonded\ (on\ Cs)}$−Th−$F_{nonbonded}$ (deg)	110.2	109.1	
Th−F sym str (a')		580.2 (55)	
Th−F asym str (a'')		534.3 (206)	528
Th−F asym str (a')		531.1 (166)	528
F−F str (a')		457.4 (44)	
	ThF_5^-(D_{3h} $^1A_1'$)		
r(Th−F_{ax}) (Å)	2.194	2.194	
r(Th−F_{eq}) (Å)	2.183	2.190	
Th−F sym str (a_1')	534.4	523.8 (0)	
Th−F_{eq} asym str (e')	463.5	452.5 (242)	460
Th−F_{ax} asym str (a_2'')	451.7	446.1 (323)	460
Th−F sym str (a_1')	426.7	415.6 (0)	

[a]Values in parentheses are IR intensities (km/mol).

Table 3. Calculated Reaction Enthalpies (kcal/mol) at 298 K for the Lowest-Energy Conformer Involved in These Matrix Isolation Experiments

reaction no.	reaction	B3LYP/aug-cc-pVTZ/ECP	CCSD(T)/aug-cc-pVTZ/ECP
1	Th + F → ThF	−156.1	−153.1 (−155 ± 2)[9,10]
2	Th + F_2 → ThF_2	−292.6	−289.2
3	ThF + F → ThF_2	−164.0	−162.9
4	ThF_2 + F → ThF_3	−153.5	−153.4
5	ThF_2 + F_2 → ThF_4	−273.1	−275.4
6	ThF_3 + F → ThF_4	−156.0	−157.9
7	ThF_4 + e^- → ThF_4^-	−16.3 [0.71 eV]	−9.8 [0.42 eV]
8	ThF_5 → ThF_3 + F_2	134.6	127.6
9	ThF_5 → ThF_3^+ + F_2^-	204.3	211.1
10	ThF_5 → ThF_4 + F	15.0	5.7
11	ThF_5 + e^- → ThF_5^-	−158.1 [−6.86 eV]	−165.4 [−7.17 eV]
12	ThF_4 + F^- → ThF_5^-	−91.8	−94.7

dx.doi.org/10.1021/ic401107w | Inorg. Chem. 2013, 52, 8228−8233

2 cm^{-1} of the matrix doublet (Table 1). The weaker symmetric stretch is computed to be 4 cm^{-1} higher with 10% of the strongest band intensity, which is too weak to observe here. The 575 cm^{-1} band was labeled ThF_2 in Figure 1 of our report on the reaction of Th with NF_3 where N−ThF_3 was the major product with a strong antisymmetric ThF_3 subunit stretching absorption at 525 cm^{-1}.[12] At that time, it was thought that the much weaker (calculations predict 8%) symmetric mode might be covered by the ThF_2 band and 575 cm^{-1} was also listed in the tables for this weaker symmetric mode. Further examination of our Th + NF_3 reaction spectra reveals a weaker band at 566 cm^{-1}, which is tentatively assigned to this weaker mode for N−ThF_3. Observation of the same (575.9, 575.1) cm^{-1} band in Th experiments with F_2, NF_3, OF_2, and HF and our frequency calculations demonstrate that this absorption is due to ThF_2. The slight increase of these bands upon annealing to 20 K suggests that the Th + F_2 reaction is spontaneous, which is consistent with the large negative energy for reaction 2 (Table 3).

Our CCSD(T) calculations predict ThF_3 to be a trigonal-planar radical with a very strong antisymmetric stretching fundamental at 537 cm^{-1} and no symmetric-mode intensity as long as the radical remains planar. Thus, both the 531.0 and 528.4 cm^{-1} bands, just above this mode at 525 cm^{-1} for N−ThF_3,[12] merit consideration for ThF_3 itself. Note that the latter band is a weak shoulder on the former band using 0.5% F_2 and the former band is a weak shoulder on a much stronger latter band with 1% F_2 (Figure 1). Then note that only the 531.0 cm^{-1} band is observed upon sample deposition with the NF_3, OF_2 and HF reagents, where the ablation plume photolysis byproduct F_2 concentration is very low; however, final annealing produces a weak 528.2 or 528.4 cm^{-1} satellite peak (Figure 2). This and the understanding that molecular perturbations usually red shift isolated molecule frequencies lead us to assign the 531.0 cm^{-1} band to isolated ThF_3 and the 528.4 cm^{-1} band for ThF_3 perturbed by a fluorine molecule, the most abundant molecule present in the Ar/F_2 matrix samples. Our B3LYP calculations predict a 3 cm^{-1} red shift for this interaction. The ThF_3 radical is probably made here by the F-atom reaction with ThF_2, reaction 4 in Table 3. The major product in these experiments, ThF_4, can be made by both the F-atom and molecule reactions 5 and 6 in Table 3. It is interesting that the first F-atom elimination energies for $ThF_{1,2,3,4}$ are nearly the same, but this is highest for ThF_2 (Table 3), as is its stretching frequency.

Our DFT B3LYP/aug-cc-pVTZ-ECP calculations showed that the approach of F_2 to ThF_3 on the C_3 axis leads directly to ThF_4 and an F atom, but if the F−F molecule is not restricted to this axis, it converges without barrier to the C_s side-bound structure. We found no minimum for an end-bound structure. A sideways approach forms a (C_s $^2A''$) (ThF_3)(F_2) complex very exothermically, reaction 8 in Table 3. On the basis of the geometry parameters, natural charge analysis,[32] and the spin density (Figure 3), (ThF_3)(F_2) is best written as [ThF_3^+][F_2^-]. The calculated frequencies for the ground state (C_s $^2A''$) [ThF_3^+][F_2^-] complex are given in Table 2, and the structure is illustrated in Figure 3. We used the B3LYP/aug-cc-pVTZ/ECP calculation frequency predictions for this larger open-shell molecule because of the computational cost at the CCSD(T) level. The good agreement between the CCSD(T) and DFT/B3LYP results for the frequencies in Table 1 and for the geometries in Table 2 shows that the DFT frequencies are reliable. We assign the 528.4 cm^{-1} band (3 cm^{-1} full-width at half-maximum) to the strong antisymmetric stretching mode(s) for the ThF_3 subunit in the [ThF_3^+][F_2^-] complex, which are predicted by DFT to be separated by 3 cm^{-1} and would be degenerate under 3-fold symmetry. Although the ThF_3 subunit in the [ThF_3^+][F_2^-] complex is nonplanar, the symmetric mode associated with the ThF_3 subunit is expected to have a small IR intensity, and this weaker mode is not observed. Note that our calculations predict the symmetric mode to be near 580 cm^{-1} with ∼15% of the total antisymmetric-mode intensities at 534 and 531 cm^{-1} (Table 2). The weaker F−F stretching mode calculated at 457 cm^{-1} is not observed because this band may be broad and matrix-shifted too low for detection.

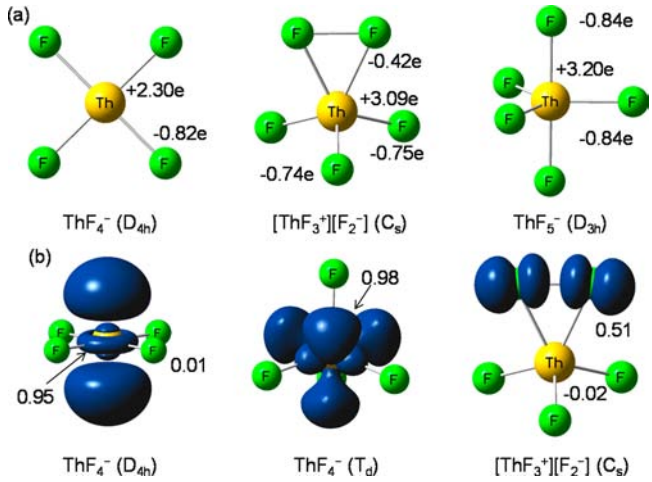

Figure 3. (a) Structures and natural charges for the lowest-energy conformers of ThF_4^-, [ThF_3^+][F_2^-], and ThF_5^- and (b) spin densities for ThF_4^-(D_{4h}) (0.95 on Th), [ThF_3^+][F_2^-] (0.51 on each F in the F_2^- fragment and −0.02 on Th), and ThF_4^-(T_d) (0.98 on Th),.

The related alkali-metal (M^+)(F_2^-) species were observed by matrix Raman spectroscopy, and the F_2^- stretching modes ranged from 452 to 475 cm^{-1} for different alkali-metal reactions with fluorine.[33] We calculated the isolated F_2^- fundamental to be at 435 cm^{-1} (ω_e = 446.6 cm^{-1} and $\omega_e x_e$ = 6.0 cm^{-1}) at the CCSD(T)/aug-cc-pVTZ/ECP level with r(F−F) = 1.927 Å.[34] It is typical for (cation)(anion) paired species to have higher anion frequencies than isolated anions, as found for [M^+][F_2^-] and the current [ThF_3^+][F_2^-] species. As another example, [M^+][F_3^-] has the antisymmetric F−F−F stretching fundamental at 550 cm^{-1} for M = K, Rb, Cs relative to an isolated F_3^- value at 510 cm^{-1} in solid argon.[17,35] It is useful to note a weak F_3^- band at 510 cm^{-1} in our solid argon experiments, which verifies the presence of laser-ablated electrons and F^- in fluorine bearing argon condensed with metal ablation.[19] Further support for our observation of the [ThF_3^+][F_2^-] complex in these fluorine-rich samples is the high stability of ThF_3(F_2) with respect to dissociation to ThF_3 + F_2 (reaction 8, Table 3). The Th−F bond in ThF_4 is very strong (158 kcal/mol; reaction 6, Table 3), so it is not surprising that this ThF_5 isomer is stable by only 6 kcal/mol with respect to the ThF_4 + F asymptote (reaction 10, Table 3). Thus, ThF_5 can only be stabilized at low temperatures, such as those in our matrix isolation experiments.

Our calculations further show that electron capture by [ThF_3^+][F_2^-] is a highly exothermic process (reaction 11, Table 3), leading to the trigonal-bipyramidal ThF_5^- anion with strong antisymmetric Th−F stretching modes predicted in the 446−464 cm^{-1} range (Table 2). The broader 460 cm^{-1} band

dx.doi.org/10.1021/ic401107w | Inorg. Chem. 2013, 52, 8228−8233

shows the decrease upon annealing expected for an isolated molecular ion, and its increase upon UV irradiation, *with destruction of the F_3^- band at 510 cm^{-1}*, is expected for the more stable anion. Thus, the 460 cm^{-1} band is assigned to the ThF_5^- anion, and it probably contains the absorptions for both antisymmetric Th−F stretching modes. Another highly exothermic process possible here is fluoride-anion capture by ThF_4, reaction 12 in Table 3. As noted above, observation of the F_3^- band provides evidence for F^- reactions in these experiments because the fluoride affinity of F_2 is 23 kcal/mol.[17]

Similar experiments with U and F_2 produced strong UF_6 and weaker UF_6^- anion absorptions at 620 and 520 cm^{-1}.[36,37] The electron affinity of ThF_4 is much smaller than that of UF_6, only 0.42 eV (reaction 7 in Table 3), and there are two ThF_4^- structures that are very close in energy. The lowest-energy structure is the planar D_{4h} structure.[38] The D_{4h} conformer has a predicted very strong e_u mode at 456 cm^{-1}. It is possible that broad absorption near 450 cm^{-1} is due to ThF_4^-, formed through electron capture by the major reaction product ThF_4. It is interesting to note that this possible frequency ratio for the strongest mode of the D_{4h} ThF_4 anion and the corresponding neutral, 450/521 = 0.86, is almost the same as that for the UF_6 anion and the neutral, 520/620 = 0.84. The T_d structure of ThF_4^- is 2.9 kcal/mol higher in energy at the CCSD(T)/aug-cc-pVTZ/ECP level and only 0.5 kcal/mol higher at the DFT/B3LYP level. The intense band for T_d ThF_4^- is predicted to be at 480 cm^{-1} at the DFT/B3LYP level.

CONCLUSIONS

We have shown that reactions of laser-ablated Th with F_2 produce the expected small thorium fluoride molecules ThF, ThF_2, ThF_3, and ThF_4 on the basis of the behavior of their argon matrix IR spectra upon increasing sample concentration, annealing, and irradiation, the use of complementary NF_3, OF_2, and HF precursor reactions, and a comparison with frequencies calculated by the CCSD(T) and DFT/B3LYP levels using the aug-cc-pVTZ/ECP basis set. Additional lower-frequency absorptions are assigned to the thorium pentafluoride species $[ThF_3^+][F_2^-]$ and ThF_5^-, which are formed in highly exothermic reactions. This is the first characterization of new pentacoordinated thorium species including the stable molecular cation−molecular anion $[ThF_3^+][F_2^-]$ and the isolated ThF_5^- anion. We believe that it will be possible to prepare the ThF_5^- anion with an appropriate stabilizing cation in a solid-state compound.

ASSOCIATED CONTENT

Supporting Information

Complete author lists for refs 20 and 21, figures of IR spectra for Th with HF and higher-concentration F_2 reaction products, optimized Cartesian *x*, *y*, and *z* coordinates in angstroms for ThF_5, total energies at the CCSD(T) and DFT/B3LYP levels in atomic units, and the complete list of vibrational frequencies in reciprocal centimeters. This material is available free of charge via the Internet at http://pubs.acs.org.

AUTHOR INFORMATION

Corresponding Author

*E-mail: lsa@virginia.edu (L.A.), dadixon@bama.ua.edu (D.A.D.).

Notes

The authors declare no competing financial interest.

ACKNOWLEDGMENTS

We gratefully acknowledge financial support from the DOE Office of Science, Basic Energy Sciences, supported by DOE Grant DE-SC0001034 (L.A.) and the BES SISGR program in actinide sciences (D.A.D.). D.A.D. thanks the Robert Ramsay Fund at the University of Alabama and Argonne National Laboratory for partial support. L.A. appreciates valuable assistance with the higher-fluorine-concentration experiments and helpful discussions with J. Metzger, T. Vent-Schmidt, and S. Riedel at the University of Freiburg.

REFERENCES

(1) Grenthe, I.; Drożdżyński, J.; Fujino, T.; Buck, E. C.; Albrecht-Schmitt, T. E.; Wolf, S. F. Uranium. In *The Chemistry of the Actinide and Transactinide Elements*; Morss, L. R., Edelstein, N. M., Fuger, J., Eds.; Springer: Dordrecht, The Netherlands, 2006; pp 253−698.
(2) (a) McDowell, R. S.; Asprey, L. B.; Paine, R. T. *J. Chem. Phys.* **1974**, *61*, 3571−3580. (b) Grzybowski, J. M.; Andrews, L. *J. Chem. Phys.* **1978**, *68*, 4540−4545.
(3) Beauchamp, J. L. *J. Chem. Phys.* **1976**, *64*, 929−935.
(4) Compton, R. N. *J. Chem. Phys.* **1977**, *66*, 4478−4485.
(5) de Jong, W. A.; Nieuwpoort, W. C. *Int. J. Quantum Chem.* **1996**, *58*, 203−216.
(6) Buchler, A.; Berkowitz-Mattuck, J. B.; Dugre, D. H. *J. Chem. Phys.* **1961**, *34*, 2202−2203.
(7) Buchmarina, V. N.; Gerasimov, A. Yu.; Predtechenskii, Yu. B.; Shklyarik, V. G. *Opt. Spectrosc. (USSR)* **1992**, *72*, 38−40.
(8) Konings, R. J. M.; Hildenbrand, D. L. *J. Alloys Compd.* **1998**, *271*−*273*, 583−586.
(9) Barker, B. J.; Antonov, I. O.; Heaven, M. C.; Peterson, K. A. *J. Chem. Phys.* **2012**, *136*, 104305.
(10) Lau, K. H.; Brittain, R. D.; Hildenbrand, D. L. *J. Chem. Phys.* **1989**, *90*, 1158−1164.
(11) Gong, Y.; Wang, X. F.; Andrews, L.; Schlöder, T.; Riedel, S. *Inorg. Chem.* **2012**, *51*, 6983−6991.
(12) Wang, X. F.; Andrews, L. *Dalton Trans.* **2009**, 9260−9265.
(13) Andrews, L.; Gong, Y.; Liang, B.; Jackson, V. E.; Flamerich, R.; Li, S.; Dixon, D. A. *J. Phys. Chem. A* **2011**, *115*, 14407−14416.
(14) Zhou, M. F.; Andrews, L. *J. Chem. Phys.* **1999**, *111*, 11044−11049.
(15) Souter, P. F.; Kushto, G. P.; Andrews, L.; Neurock, M. *J. Phys. Chem. A* **1997**, *101*, 1287−1291.
(16) Andrews, L.; Citra, A. *Chem. Rev.* **2012**, *102*, 885−911.
(17) Andrews, L. *Chem. Soc. Rev.* **2004**, *33*, 123−132.
(18) Andrews, L.; Cho, H.-G. *Organometallics* **2006**, *25*, 4040−4053.
(19) Riedel, S.; Köchner, T.; Wang, X. F.; Andrews, L. *Inorg. Chem.* **2010**, *49*, 7156−7164.
(20) Frisch, M. J.; Trucks, G. W.; Schlegel, H. B.; Scuseria, G. E.; Robb, M. A.; Cheeseman, J. R.; Scalmani, G.; Barone, V.; Mennucci, B.; Petersson, G. A.; et al. *Gaussian 09*, revision B.01; Gaussian, Inc.: Wallingford, CT, 2009.
(21) Knowles, P. J.; Manby, F. R.; Schütz, M.; Celani, P.; Knizia, G.; Korona, T.; Lindh, R.; Mitrushenkov, A.; Rauhut, G.; Adler, T. B.; et al. *MOLPRO, version 2010.1, a package of ab initio programs*. See http://www.molpro.net.
(22) Becke, A. D. *J. Chem. Phys.* **1993**, *98*, 5648−5652.
(23) Lee, C.; Yang, W.; Parr, R. G. *Phys. Rev. B* **1988**, *37*, 785−789.
(24) Purvis, G. D., III; Bartlett, R. J. *J. Chem. Phys.* **1982**, *76*, 1910−1918.
(25) Raghavachari, K.; Trucks, G. W.; Pople, J. A.; Head-Gordon, M. *Chem. Phys. Lett.* **1989**, *157*, 479−483.
(26) Watts, J. D.; Gauss, J.; Bartlett, R. J. *J. Chem. Phys.* **1993**, *98*, 8718−8733.
(27) (a) Deegan, M. J. O.; Knowles, P. J. *Chem. Phys. Lett.* **1994**, *227*, 321−326. (b) Rittby, M.; Bartlett, R. J. *J. Phys. Chem.* **1988**, *92*, 3033−3036.

(28) Kendall, R. A.; Dunning, T. H., Jr.; Harrison, R. J. *J. Chem. Phys.* **1992**, *96*, 6796−6806.
(29) (a) Küchle, W.; Dolg, M.; Stoll, H.; Preuss, H. *J. Chem. Phys.* **1994**, *100*, 7535−7542. (b) Institut für Theoretische Chemie Universität Stuttgart, http://www.theochem.uni-stuttgart.de/pseudopotentials/index.en.html. (c) Cao, X.; Dolg, M.; Stoll, H. *J. Chem. Phys.* **2003**, *118*, 487−496. (d) Cao, X.; Dolg, M. *J. Mol. Struct. (THEOCHEM)* **2004**, *673*, 203−209.
(30) Gong, Y.; Andrews, L.; Jackson, V. E.; Dixon, D. A. *Inorg. Chem.* **2012**, *51*, 11055−11060.
(31) Sansonetti, J. E.; Martin, W. C. *J. Phys. Chem. Ref. Data* **2005**, *34*, 1559−2259. See also http://physics.nist.gov/PhysRefData/Handbook/Tables/iridiumtable5.htm.
(32) Reed, A. E.; Curtiss, L. A.; Weinhold, F. *Chem. Rev.* **1988**, *88*, 899−926. Reed, A. E.; Weinstock, R. B.; Weinhold, F. *J. Chem. Phys.* **1985**, *83*, 735−746. Weinhold, F.; Landis, C. R. *Valency and Bonding*; Cambridge University Press: Cambridge, U.K., 2005. Glendening, E. D., Reed, A. E., Carpenter, J. E., Weinhold, F. *NBO*, version 3.1; Department of Chemistry, University of Wisconsin—Madison: Madison, WI, 1988.
(33) Howard, W. F., Jr.; Andrews, L. *J. Am. Chem. Soc.* **1973**, *95*, 3045−3046.
(34) DFT/B3LYP gives a longer bond distance of 2.006 Å and a lower ω_e of 357 cm^{-1}.
(35) Ault, B. S.; Andrews, L. *J. Am. Chem. Soc.* **1976**, *98*, 1591−1592.
(36) Hunt, R. D.; Thompson, C.; Hassanzadeh, P.; Andrews, L. *Inorg. Chem.* **1994**, *33*, 388−391 and references cited therein.
(37) Kunze, K. R.; Hauge, R. H.; Hamill, D.; Margrave, J. L. *J. Chem. Soc., Dalton Trans.* **1978**, 433−440.
(38) There are two small imaginary frequencies at both the CCSD(T) (46*i* and 52*i*) and DFT/B3LYP levels. Following these frequencies led to a higher-energy C_{4v} structure with a single imaginary frequency or to the T_d structure.